Eur. Phys. J. A **15**, 209–212 (2002)
DOI 10.1140/epja/i2001-10256-2

THE EUROPEAN PHYSICAL JOURNAL A

Microscopic structure of superdeformed states in Th, U, Pu and Cm isotopes with Gogny force

M. Girod[1,a], J. Libert[2], J.-P. Delaroche[1], and P. Romain[1]

[1] CEA/DIF, DPTA/SPN, Boîte Postale 12, 91680 Bruyères-le-Châtel, France
[2] Institut de Physique Nucléaire Centre National de la Recherche Scientifique-IN2P3, F-91406 Orsay, France

Received: 21 March 2002 /
Published online: 31 October 2002 –

Abstract. The structure properties of the even-even nuclei ^{226,228,230,232,234}Th, ^{230,232,234,236,238,240}U, ^{240,242,244,246}Pu, and ^{242,244,246,248}Cm have been investigated at normal and superdeformed shapes in microscopic mean-field calculations based on Gogny force. Collective levels are predicted from constrained Hartree-Fock-Bogoliubov and configuration mixing calculations. Two quasiparticle states are also predicted from blocking calculations for neutron and proton configurations. Predictions are shown and compared with experimental data at superdeformed shapes.

PACS. 21.60.Ev Collective models – 21.60.Jz Hartree-Fock and random-phase approximations – 23.20.Lv Gamma transitions and level energies – 27.90.+b $A \geq 220$

1 Introduction

After the discovery of fission isomers and detailed spectroscopic studies of superdeformed (SD) isomeric states in several actinide nuclei [1,2], the main trust has been put on SD nuclei with masses $A < 200$. For these nuclei, stability of secondary minima at large elongation in their potential energy surfaces (PESs) is gained only through increasing rotational frequencies that may be obtained using fusion-evaporation reactions between heavy ions at energies close to the Coulomb barrier. It is only recently that SD phenomena have been revisited in the actinide region using traditional probes together with experimental set-up of the new generation. Many SD bands have been identified in measurements for the Pu region [3–5].

Since microscopic mean-field methods have shown good predictive power in spectroscopic studies of even-even nuclei at normal and large elongations in the $A \simeq 190$ mass region [6], we have found it interesting to investigate by this mean both $\pi = +$ collective quadrupole levels and $\pi = \pm$ two quasiparticle (2qp) excitations, not only for ^{240}Pu but also for many even-even Th, U, Pu and Cm isotopes. This large-scale model study provides information on shell structure and shape evolutions at large deformation as functions of proton and neutron numbers. As such, this information may also serve to establish reaction models on microscopic grounds especially for neutron-induced fission at low energy [1].

[a] e-mail: michel-g.girod@cla.tr

Section 2 includes a short presentation of i) the constrained Hartree-Fock-Bogoliubov (HFB) method used to predict PES landscapes, ii) the configuration mixing method for the prediction of $\pi = +$ quadrupole collective levels, and iii) the blocking method to predict $\pi = +$ and $\pi = -$2qp states at SD shapes. Our predictions are discussed in sect. 3 and compared with recent experimental data. The sole input to these calculations is the finite-range, density-dependent D1S Gogny force [7].

2 Microscopic models

2.1 Potential energy surfaces

They are calculated as functions of axial (q_0) and triaxial (q_2) quadrupole deformations from solving by iterations the constrained HFB equations, namely

$$\delta\langle\Phi_q|\hat{H} - \lambda_0\hat{Q}_0 - \lambda_2\hat{Q}_2 - \lambda_Z\hat{Z} - \lambda_N\hat{N}|\Phi_q\rangle = 0, \quad (1)$$

and

$$\langle\Phi_q|\hat{N}|\Phi_q\rangle = N, \qquad \langle\Phi_q|\hat{Z}|\Phi_q\rangle = Z, \qquad \langle\Phi_q|\hat{Q}_i|\Phi_q\rangle = q_i. \quad (2)$$

In this equation, Φ_q is the qp vacuum, λ_i ($i = 0, 2, Z, N$) are Lagrange multipliers, $\hat{Q}_i$ ($i = 0, 2$) external fields generating axial and triaxial deformations, and $\hat{Z}$ and $\hat{N}$ are the proton and neutron number operators, respectively. Furthermore $\hat{H}$ is the nuclear Hamiltonian. The quadrupole coordinates q_0 and q_2 are related to the

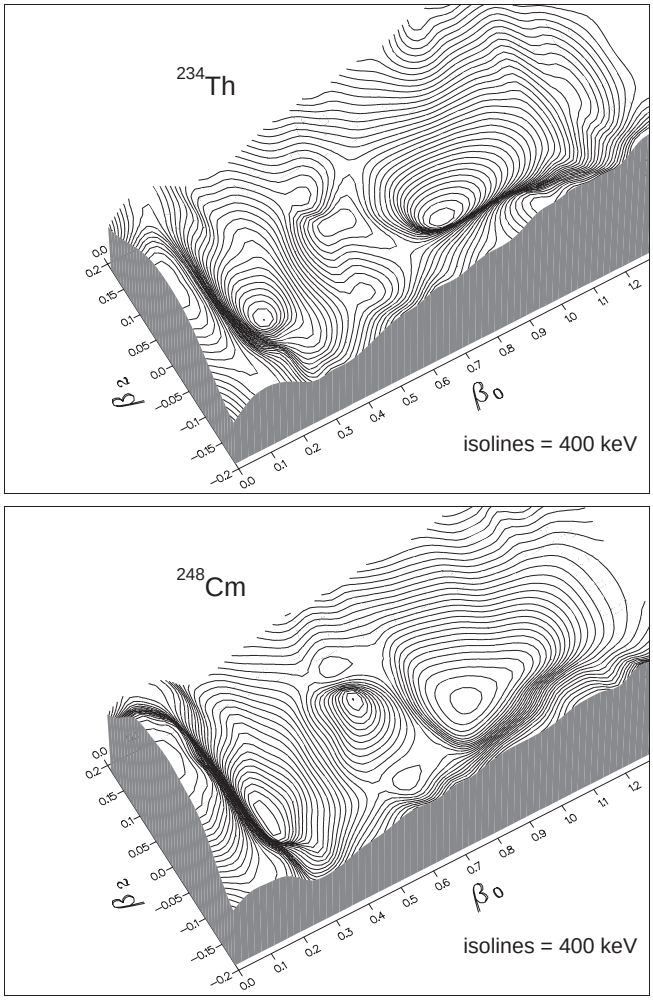

Fig. 1. Potential energy surfaces (in MeV) for ^{234}Th and ^{248}Cm as functions of the Cartesian coordinates β_0 and β_2. Zero-point energy corrections are included [6]. The lines are separated by 400 keV from each other. For more details, see text.

polar Bohr deformations β and γ through the usual relationships [6]. Once the set of eq. (1) is solved, the potential energy surface is obtained either as $V(q) = \langle \Phi_q | \hat{H} | \Phi_q \rangle$, with $q = (q_0, q_2)$, or $V(\beta, \gamma)$ through the $(q_0, q_2) \rightarrow (\beta, \gamma)$ transformation, or $V(\beta_0, \beta_2)$, where $\beta_0 = \beta \cos\gamma$ and $\beta_2 = \beta \sin\gamma$ are Cartesian coordinates.

2.2 Configuration mixing calculations

These are used to predict the $\pi = +$ quadrupole collective levels that are eigenstates of a collective Hamiltonian $\hat{\mathcal{H}}_{\rm coll}$ built from potential energy surfaces, moments of inertia, and collective masses [6]. $\hat{\mathcal{H}}_{\rm coll}$ is solved numerically employing a two-center basis.

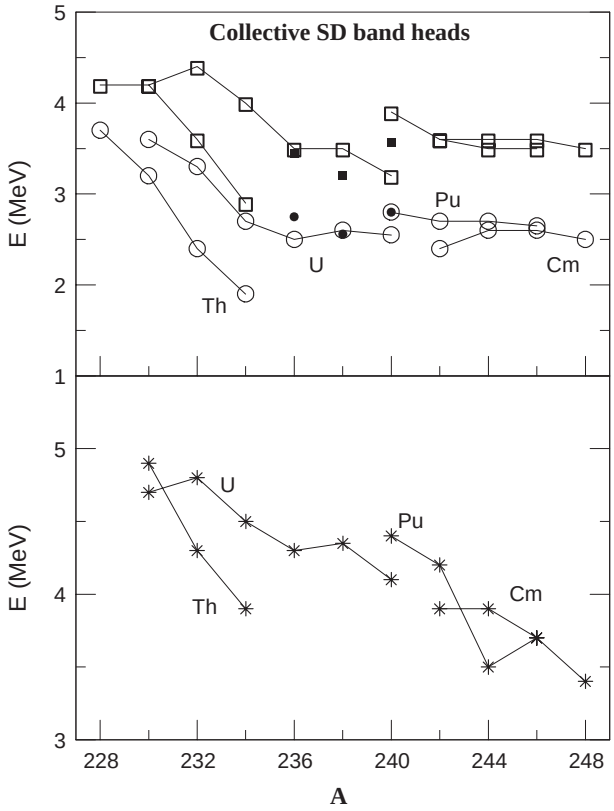

Fig. 2. Excitation energies of $\pi = +$ collective head levels at SD shapes. In the upper panel are shown our predictions represented as open circles ($0^+_{\rm SD}$ levels) and open squares ($0^{+\prime}_{\rm SD}$ levels). The full circles and squares are for respective experimental SD values available for ^{236}U, ^{238}U and ^{240}Pu. The lower panel includes our predictions (stars) for the $2^+_{\rm SD}$ "γ" vibrations.

2.3 Blocking calculations

The proton and neutron 2qp states are predicted using blocking calculations here performed without breaking time reversal symmetry. With this approximation, the signature partner pairs are degenerated in energy. The 2qp levels are obtained from solving a set of equations similar to eq. (1), in which the qp vacuum Φ_q is replaced by a new trial function

$$\left|\Phi'_q\right\rangle = \eta_i^+ \eta_j^+ \left|\Phi_q\right\rangle, \qquad (3)$$

where η_i^+ is a 1qp creation operator, and i an index for blocked 1qp orbitals.

3 Results

3.1 PES landscapes

The PESs calculated in the domain defined by $0 \leq \beta \leq 1.4$ and $0^\circ \leq \gamma \leq 60^\circ$ display deep minima at normal deformation (ND) with $\beta_{\rm I} \simeq 0.3$ and $\gamma_{\rm I} = 0^\circ$, and secondary minima characterized by $\beta_{\rm II} \simeq 0.6 - 0.9$ and $\gamma_{\rm II} = 0^\circ$. The inner potential barrier (B) is always high in energy with respect to the ND potential minimum, with typical axial

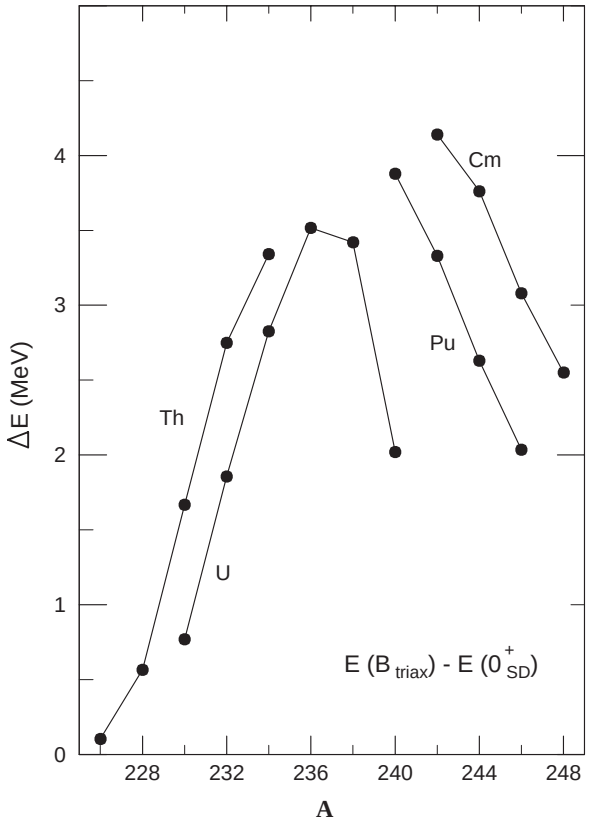

Fig. 3. Predicted energy differences between $E(B_{\rm triax})$ and $E(0^+_{\rm SD})$.

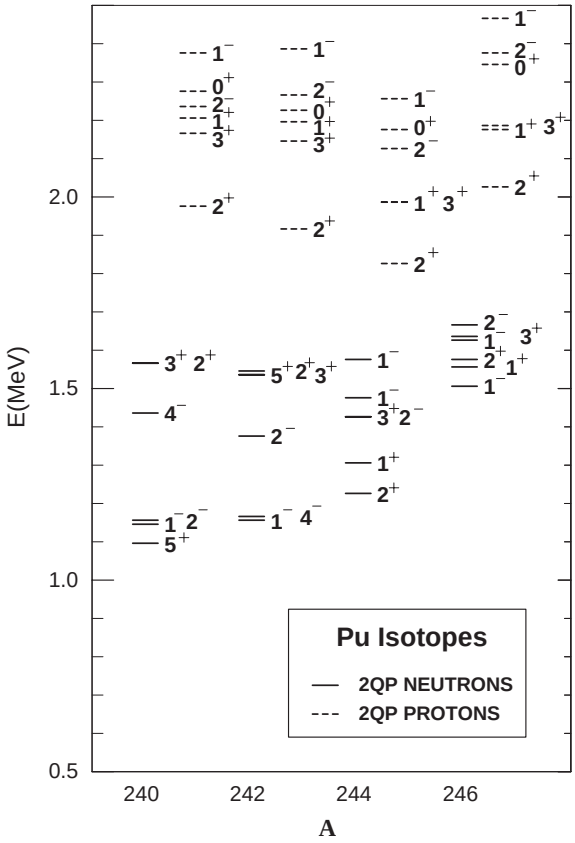

Fig. 4. First 2qp neutron (solid lines) and proton (dashed lines) states predicted for plutonium isotopes.

values $E(B_{\rm ax}) \simeq$ 6–10 MeV. For all nuclei are observed triaxial ($\gamma \simeq 5°$) saddles between ND and SD potential minima, with energies $E(B_{\rm triax})$ up to a few MeV lower than $E(B_{\rm ax})$'s. These saddles may also display local minima 500 keV deep, for instance for ^{246}Pu and ^{248}Cm.

Illustrations for typical PES landscapes expressed in terms of Cartesian coordinates, are shown in fig. 1 for ^{234}Th and ^{248}Cm. As can be seen, the SD potential for ^{234}Th is stiffer along the (β_0, β_2) coordinates than for ^{248}Cm. This feature suggests that excitation energy of vibrational SD states relative to the SD ground states will be lower for ^{248}Cm.

The SD potential minima are a few MeV deep with respect to either saddles or axial barriers. However, this minimum is not deep enough in ^{226}Th to sustain an $0^+_{\rm SD}$ isomeric level. This property suggests that shape isomerism in the actinide region is unlikely to take place for neutron-deficient nuclides with neutron numbers ≤ 136.

3.2 Collective $\pi = +$ SD states

The head levels of the "ground-state" ($0^+_{\rm SD}$), one-phonon "β" ($0^{+\prime}_{\rm SD}$), and one-phonon "γ" ($2^+_{\rm SD}$) bands are shown as open circles, open squares and stars, respectively, in fig. 2. For comparison, the upper panel of fig. 2 includes data for $0^+_{\rm SD}$ (full circles) and $0^{+\prime}_{\rm SD}$ (full squares) head band levels as inferred from measurements for ^{236}U, ^{238}U and ^{240}Pu [3,4,8]. As can be seen, the predictions match the data to within 400 keV, which is gratifying considering the parameter free character of our microscopic models. In the lower panel of fig. 2 the $2^+_{\rm SD}$ levels predictions are shown. The gradual lowering in energy of these states with increasing mass stems from the gradual softening of SD potentials with respect to the triaxial degree of freedom. This mode gets so soft in ^{248}Cm that the $2^+_{\rm SD}$ level is predicted as the lowest one-phonon excitation.

3.3 Energy localization of $0^+_{\rm SD}$ states

It is useful to consider how high in energy the predicted $0^+_{\rm SD}$ isomers are placed with respect to the height of triaxial saddles, because the energy difference $\Delta E = E(B_{\rm triax}) - E(0^+_{\rm SD})$ provides us with qualitative information on lifetime (τ_γ) associated with the γ-decay of $0^+_{\rm SD}$ levels towards ND states. The more the gap ΔE is large, the more τ_γ is likely to be long. From fig. 3, it is seen that this gap takes on maximum values for ^{234}Th, ^{236,238}U, ^{240}Pu and ^{242}Cm, that is for $N = 144$, 146.

3.4 2qp states in SD potentials

In fig. 4 the first 2qp states for plutonium isotopes are shown. As can be seen, the 2qp excitation energies are

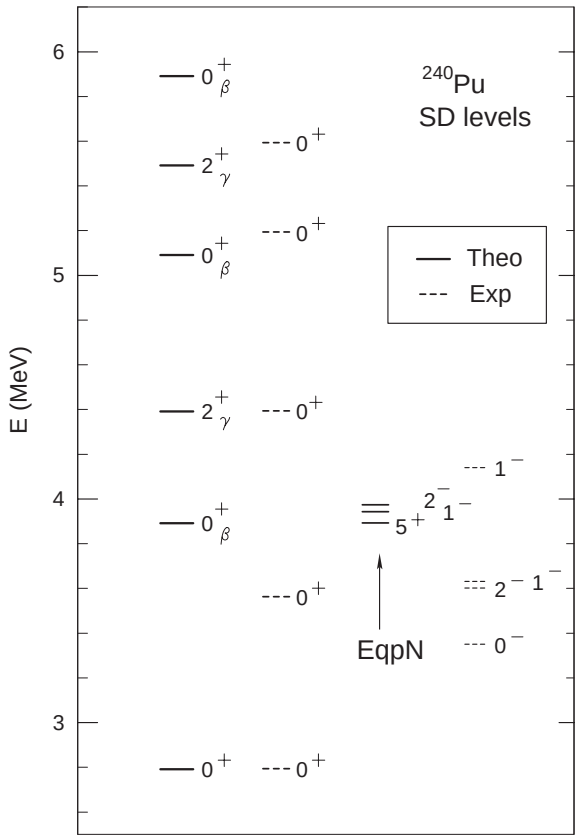

Fig. 5. SD band head levels in ^{240}Pu. Comparison between our predicted collective and 2qp neutron excitations (solid lines) and experimental results (dashed lines) for SD levels. The three levels marked with the symbol EqpN are 2qp neutron excitations.

lowest for neutron configurations. The 2qp proton excitations are located at energies roughly two times higher than those of 2qp neutron excitations. We find the same feature for all the presently studied nuclei. Many of these 2qp neutron excitations take place in the 1–2 MeV energy range above $0^+_{\rm SD}$ states, only slightly higher in energy than the $0^+_{\rm SD}{}'$ levels shown in the top panel of fig. 2.

3.5 Spectroscopy of ^{240}Pu SD states

^{240}Pu is a nucleus for which many SD bands have recently been identified. Among the lowest ones, most of them were tentatively interpreted as built on top of octupole vibrations [3–5]. It was also suggested that three SD bands at excitation energies between 4 and 6 MeV are multiphonons of "β"-vibrational character. Furthermore, these families of SD states display a near regular spacing which would imply harmonic vibrations [3–5]. As can be seen on the left-hand side of fig. 5, these experimental results are in qualitative agreement with our predictions provided that both "β" and "γ" vibrations are considered. The right-hand side of fig. 5 also displays other SD band head levels which have been identified [3–5] as $\pi = -$ bands. Our calculations suggest that such bands might stem from 2qp neutron excitations.

4 Conclusion

A systematic structure model study of superdeformed states is underway for Th, U, Pu and Cm isotopes in our laboratories. This work is performed using self-consistent mean-field methods and extensions beyond the mean-field approximation, in which the finite-range, density-dependent D1S force is the sole input. Calculations have been performed for 19 even-even nuclides with masses $226 \leq A \leq 248$, which provide predictions for PES landscapes, shape isomers, $\pi = +$ quadrupole vibrations, and $\pi = +$ and $\pi = -$ 2qp excitations in the secondary potential minima. It is found that the inner potential barriers display minima at non-axial shapes, which suggests triaxial paths in the early stage of the cold-fission process. Furthermore, the predicted and observed shape isomers as well as "β" SD band heads for ^{236,238}U and ^{240}Pu have excitation energies in reasonably good agreement. Much more work remains to be done on the theory side for the achievement of an improved understanding of SD state and band properties in the actinide mass region. More data are also needed to challenge our model predictions.

References

1. S. Bjørnholm, J.E. Lynn, Rev. Mod. Phys. **52**, 725 (1980).
2. V. Metag, D. Habs, H.J. Specht, Phys. Rep. **65**, 1 (1980).
3. D. Pansegrau, P. Reiter, D. Schwalm. H. Bauer, J. Eberth, D. Gassmann, D. Habs, T. Härtlein, F. Köck, H.G. Thomas, Phys. Lett. B **484**, 1 (2000).
4. D. Gassmann *et al.*, Phys. Lett. B **497**, 181 (2001).
5. M. Hunyadi *et al.*, Phys. Lett. B **505**, 27 (2001).
6. J. Libert, M. Girod, J.-P. Delaroche, Phys. Rev. C **60**, 054301 (1999).
7. J.F. Berger, M. Girod, D. Gogny, Comput. Phys. Commun. **63**, 365 (1991).
8. U. Goerlach, D. Habs, V. Metag, B. Schwartz, H.J. Specht, H. Backe, Phys. Rev. Lett. **48**, 1160 (1982).